J Mol Hist (2015) 46:337–345
DOI 10.1007/s10735-015-9625-4

ORIGINAL PAPER

Atorvastatin alleviates experimental diabetic cardiomyopathy by suppressing apoptosis and oxidative stress

Ahmed A. M. Abdel-Hamid[1] · **Alaa El-Din L. Firgany**[1]

Received: 21 April 2015 / Accepted: 30 May 2015 / Published online: 4 June 2015

Abstract Diabetic hazard on the myocardium is a complication of diabetes that intensifies its morbidity and increases its mortality. Therefore, alleviation of diabetic cardiomyopathy (DCM) by a reliable drug remains a matter of interest in experimental research. The aim of this study was to explore the structural alterations in the myocardium induced by atorvastatin (ATOR) in DCM, induced by streptozotocin (STZ), along with the associated changes occurring in apoptosis and oxidative stress markers. Thirty-two rats were divided into four groups; group A (control), group B (non-diabetic, received ATOR, orally, 50 mg/kg daily), group C (DCM, received STZ 70 mg/kg, single i.p. injection) and group D (DCM + ATOR). After 6 weeks, left ventricle (LV) specimens were prepared for histological and immunohistochemical study by hematoxylin and eosin, Masson's trichrome, anti-cleaved caspase-3 stains as well as for assays of oxidative stress markers. All data were measured morphometrically and statistically analyzed. The DCM group showed disorganization of the cardiomyocytes, interstitial edema, numerous fibroblasts, significant increases in the collagen volume fraction ($p < 0.001$), cleaved caspase-3 expression % area ($p < 0.001$) and, malondialdehyde in blood ($p < 0.001$), in LV ($p < 0.05$) compared with DCM + ATOR group. The latter has LV wall thickness, relative heart weight and antioxidant activities nearly similar to the control, independent from ATOR lipid-lowering effect. Therefore, ATOR can preserve myocardial structure in DCM nearly similar to normal. This may be achieved by suppressing apoptosis that parallels the correction of the antioxidant markers, which can be considered as non-lipid lowering benefit of statins.

Keywords Diabetic cardiomyopathy · Statins · Caspase-3 · Apoptosis · Oxidative stress

Introduction

Diabetic cardiomyopathy (DCM) is characterized by ventricular dysfunction (VD) that occurs in diabetes mellitus (DM) independent of coronary artery disease (CAD), hypertension (HTN), or other cardiovascular diseases (Duncan 2011; Falcao-Pires and Leite-Moreira 2012; Palomer et al. 2013; Ouyang et al. 2014). Its prevalence ranges roughly from 14.5 to 30 % in longstanding type 1 DM (Konduracka et al. 2013; Shida et al. 2014). Moreover, 75 % of unexplained dilated CM cases were found to be diabetic (Tarquini et al. 2011).

As DCM is a major contributor to DM-related morbidity and mortality, the need to clarify mechanisms of its pathogenesis is increasing (Schilling and Mann 2012; Guleria et al. 2013; Pappachan et al. 2013; Ouyang et al. 2014).

Cardiomyocyte steatosis, apoptosis and fibrosis, are key processes in DCM. However, their underlying mechanisms are still elusive, (Picatoste et al. 2013; Ramirez et al. 2013). Cardiomyocyte apoptosis is enhanced by hyperglycemia-induced oxidative stress that activates caspase-3 activation pathways (Cai et al. 2006; Zou and Xie 2013; Ouyang et al. 2014). Caspase-3 exists as inactive precursor, procaspase-3, which is converted to active key effector, cleaved caspase-3, in apoptotic cells (Xue et al. 1996; Zidar et al. 2006).

✉ Ahmed A. M. Abdel-Hamid
drahmadabdelhamid@gmail.com

[1] Department of Histology and Cell Biology, Faculty of Medicine, Mansoura University, P.O. 35516, Mansoura, Egypt

Studies have revealed that the lipid-lowering medication, statin, has beneficial effects beyond those predicted by its cholesterol-lowering actions (Van Linthout et al. 2007). Statin is considered as a first choice drug in reducing mortality and major cardio-and cerebro-vascular events, among diabetics without CAD (Chen et al. 2012; Taylor et al. 2013). Although its beneficial effect in treatment of dyslipidemia is well-established, there is controversy regarding statin role in DCM (Chen et al. 2012; Pappachan et al. 2013).

In this study, we investigated whether ATOR can hinder the progression of DCM by a mechanism other than its lipid-lowering action and its effects on the associated apoptosis and oxidative stress which accompany the hyperglycemia-induced metabolic disturbance.

Materials and methods

Experimental animals

Adult male Sprague–Dawley rats (250 ± 20 g) were obtained from Nile Centre for Experimental Researches (NCER, Mansoura, Egypt), where the experiment was performed in its experimental animal house. Animals (n = 32) were divided equally into four groups (n = 8 each) and were maintained on 12/12 h light/dark cycle at 23 ± 2 °C room temperature. All animals received standard laboratory animal's chow and water *ad labitum* during the period of the experiment. The experimental procedures were approved by the Institutional Laboratory Animal Care and Use Committee of Mansoura Faculty of Medicine and were conducted in accordance with their guidelines.

Experimental design

While eight non-diabetic rats were considered as the control group, other eight non-diabetic rats received atorvastatin (control + ATOR group). Rats having blood glucose levels ≥300 mg/dl, 1 week after streptozotocin (STZ) injection, were selected to be the DCM group. In parallel, other eight diabetic rats that received atorvastatin starting 1 week after STZ injection, was considered as the DCM + ATOR group. STZ-induced DCM is an established model for DCM (Huynh et al. 2014), therefore DM was induced by a single injection of STZ (70 mg/kg; i.p.; Sigma Chemical Co., St. Louis, MO, USA). Atorvastatin (ATOR 20 mg tablets, Eipico, Egypt) was given in a dose of 50 mg/kg daily orally by gavage for 6 weeks. Van Linthout et al. 2007 have reported that the selected dose of ATOR has not altered the LDL-cholesterol in diabetic rats. As there was no significant difference between control and control + ATOR rats in all their data (biochemical and histological), therefore these two groups were pooled in one group (control).

Histological procedure

After 6 weeks from the start the experiment, blood was withdrawn from the animals for the biochemical analysis. Then they were sacrificed and their hearts were dissected out and weighed. Specimens from the left ventricle (LV) were transversely cut for histological, immunohistochemical, and biochemical studies. Portions from LV were fixed in 10 % buffered formalin, embedded in paraffin, and cut (3–4 μm thickness). Paraffin sections were prepared for H&E and Masson's trichrome staining.

Immunohistochemical study

Paraffin sections of the LV were immunohistochemically stained for detection of cleaved caspase-3 expression as previously reported (Lim and Lee 2012; Lim et al. 2014). Rabbit polyclonal anti-cleaved caspase-3 (1:50 dilution, Cell Signaling, Beverly, MA) was applied as a primary antibody. Sections were stained using a Vectastain Elite ABC kit (Vector Laboratories, Burlington, ON). Visualization of the immunoreaction was carried out by 3,3′-diaminobenzidine tetrahydrochloride (DAB; Roche, Mannheim, Germany). From each section, 10 fields were randomly selected and evaluated (×200 magnification). The percentage area caspase-3 per section was semi-quantitatively measured using Image-Pro Plus 6.0 software (Media Cybernetics, Bethesda, MD).

Oxidative stress assessment

Serum was separated from the collected blood for measurement of malondialdehyde (MDA) level as a marker of lipid peroxidation. In addition, portions of LV were used to determine the levels of MDA and glutathione (GSH) according to the previous guidelines (Beutler et al. 1963), the cytosolic enzyme activities of glutathione peroxidase (GPx; Paglia and Valentine 1967), glutathione reductase (GR; Long and Carson 1961) and glutathione-*S*-transferase (GST; Gawai and Pawar 1984) were also assessed.

Lipid profile assessment

Serum total cholesterol (TC), high-density lipoprotein cholesterol (HDL), low density lipoprotein cholesterol (LDL), and triglycerides (TG) were determined in the collected blood samples by RA-50 Chemistry Analyzer spectrophotometer (Bayer; Tietz et al. 2006).

Morphometric analysis

The thickness of LV wall (in μm) as well as the average diameter of the cardiomyocytes (in μm) in each H&E-stained section were determined in 20 fields (×100 magnification), by Image-J software version 1.43 (NIH, Bethesda, Maryland).

Blue-stained collagen fibers were quantified in Masson's trichrome-stained sections. The volume fraction (CVF) of the interstitial (matrix) collagen was analyzed semi-quantitatively by Image-Pro Plus 6.0 software (Media Cybernetics, Bethesda, MD) according to previously described (Sun et al. 2004; Liu et al. 2015). It was calculated as the area occupied by connective tissue divided by the sum of areas occupied by connective tissue and cardiomyocytes, with exclusion of the intramural vessels, perivascular collagen, endocardium and trabeculae.

All histological evaluations were performed by a light microscope (Olympus CX31) mounted to digital camera connected to a computer.

Statistical analysis

Values were presented as mean ± SEM. One-way ANOVA test was employed for comparisons between groups followed by Tukey test by using SPSS 16 software (Chicago, IL, USA). A value of $p < 0.05$ was considered as statistically significant (Table 1).

Results

Histological results

By H&E stain, there was marked diffuse disruption of the cardiomyocytes which became fragmented and acquired a feathery appearance in the DCM group (Fig. 1c, d) compared with the control group (Fig. 1a, b). In contrast, on accompanying ATOR with DCM (Fig. 1e), a nearly normal architecture of the cardiomyocytes was observed. Moreover, numerous coronary capillaries were detected between cardiomyocytes in the DCM + ATOR group (Fig. 1f).

Contrary to its appearance in the control (Fig. 1b) and DCM + ATOR (Fig. 1e, f) groups, the sarcoplasm of cardiomycoytes in the DCM group appeared abnormally heterogeneous with many pale areas and fewer acidophilic ones (Fig. 2b, c). In addition, leakage of edema fluid from the nearby blood vessels (Fig. 2a) along with extravasation of occasional RBCs (Fig. 2d) were noticed in the interstitium of the DCM group. The latter also displayed numerous active fibroblasts in the interstitium between cardiomyocytes (Fig. 2b) compared with control group which showed only few interstitial fibroblasts (Fig. 1b).

By Masson's trichrome stain, marked increase in the interstitial collagen deposition between cardiomyocytes was obviously seen in the DCM group (Fig. 3b) unlike the DCM + ATOR (Fig. 3c) group which displayed minimal interstitial collagen nearly similar to that of the control group (Fig. 3a).

Immunohistochemical results

By anti-cleaved caspase-3 immunostain, evident increase in the caspase-3 expression was observed in the sarcoplasm of cardiomyocytes of the DCM group (Fig. 4b) compared with the minimal expression detected in the control (Fig. 4a) and DCM + ATOR (Fig. 4c) groups.

Biochemical assays results

Significant increases in BG ($p < 0.001$), TC, LDL, TG ($p < 0.05$) were detected in the DCM and DCM + ATOR groups compared with the control group without significant change in HDL (Table 2).

In addition, there was a significant increase in the oxidative stress marker, MDA, in both serum ($p < 0.001$) and heart ($p < 0.05$) of DCM group compared with control and DCM + ATOR groups. However, significant

Table 1 Body (BW), heart (HW), relative heart weights (RHW = HW/BW), LV wall thickness (μm), and cardiomyocytes diameter (μm) in various groups

	Control	DCM	DCM + ATOR
BW (g)	250 ± 20	140 ± 35**	152 ± 42**
HW (mg)	577 ± 0.43	448 ± 0.62*	366 ± 0.84*
RHW (mg/g)	2.30 ± 0.14	3.20 ± 0.17*,#	2.41 ± 0.12
LV wall thickness (μm)	3986 ± 172.43	4724 ± 196.82*,#	4112 ± 124.37
Cardiomyocyte diameter (μm)	12.82 ± 0.41	12.67 ± 0.36	13.24 ± 0.34

Values are mean ± SEM

* $p < 0.05$; ** $p < 0.001$ versus control group

# $p < 0.05$ versus DCM + ATOR group

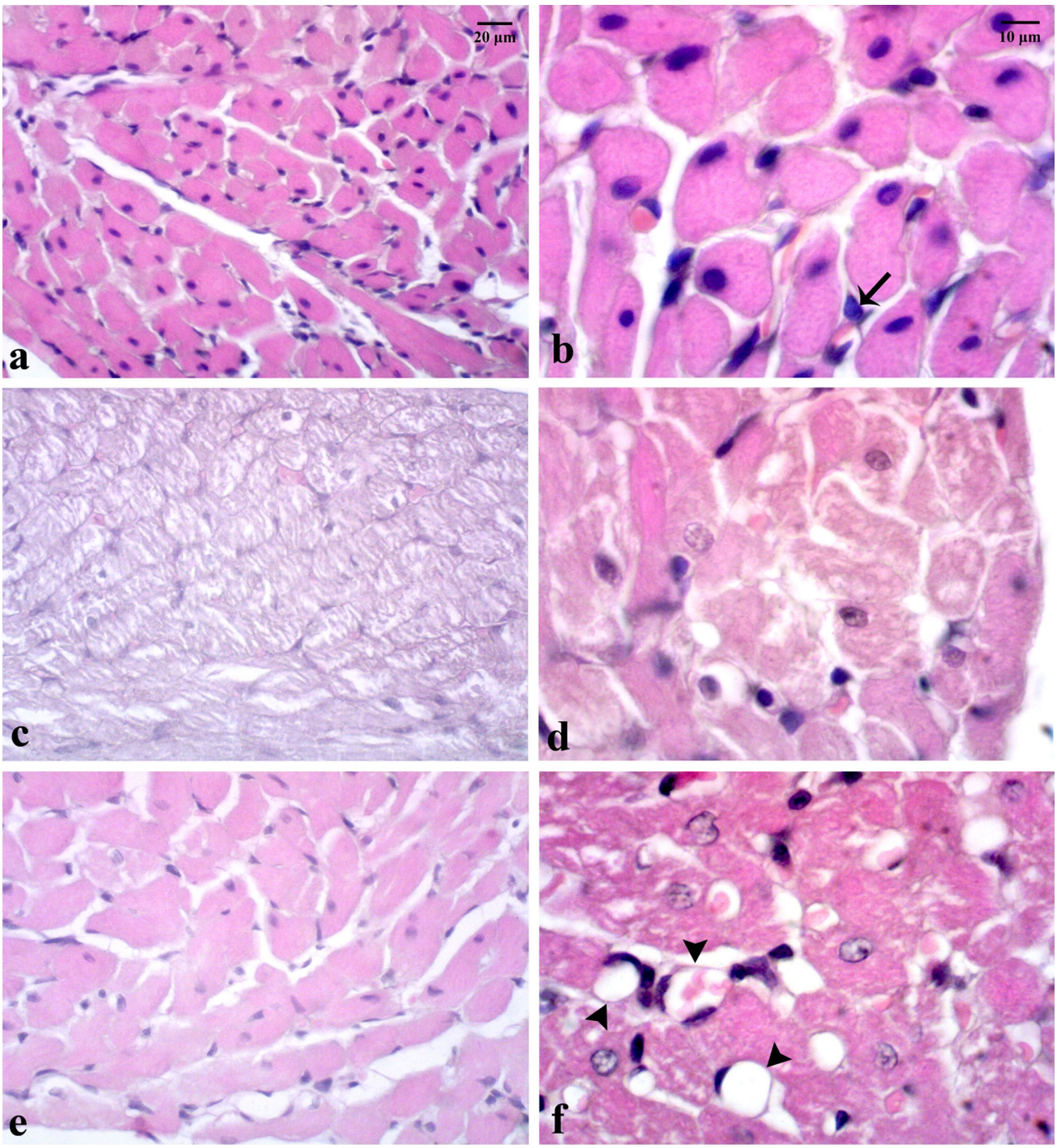

Fig. 1 Representative photomicrographs of LV in all groups stained with H&E. Disruption of the cardiomyocytes is evident in the DCM group (**c**, **d**) compared with the control (**a**, **b**) and DCM + ATOR (**e**, **f**) groups. The latter shows an increase in the capillary number (*arrow heads*) between the cardiomyocytes. Only few fibrocytes (*arrow*) are seen between cardiomyocytes of the control group (H&E **a**, **c**, **e** ×400, *Scale bar* = 20 µm; **b**, **d**, **f** ×1000, *Scale bar* = 10 µm)

decreases in the values of antioxidant markers, including the non-enzymatic, GSH ($p < 0.05$) and the enzymatic ones; GPx, GR, GST were noticed in the DCM group compared with the control and DCM + ATOR groups (Table 3).

Morphometric, body and heart weights results

There was a significant decrease in the BW ($p < 0.001$) and the HW ($p < 0.05$) of both the DCM and DCM + ATOR groups compared with the control group. On the other hand,

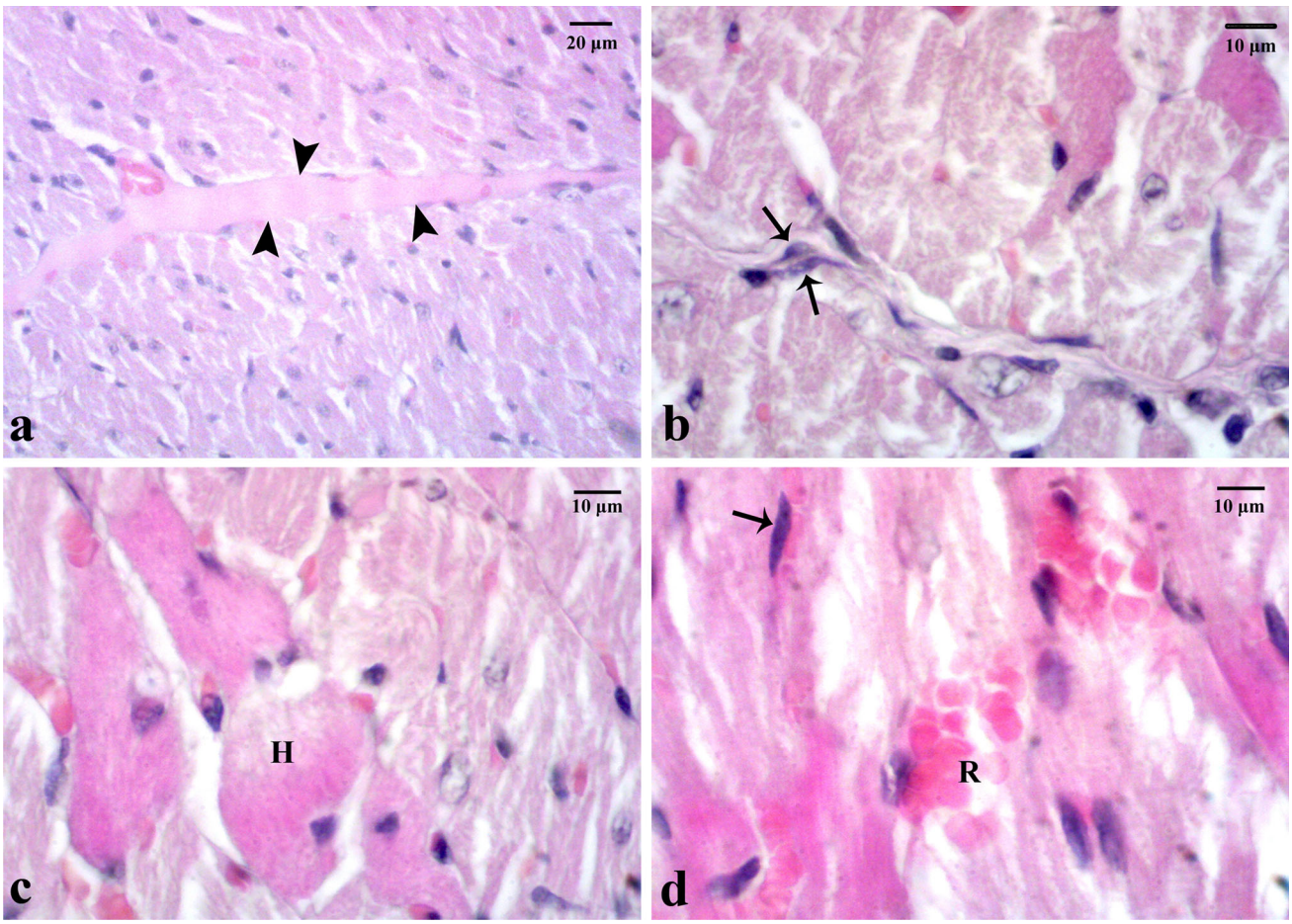

Fig. 2 Representative photomicrographs of LV in DCM group stained with H&E. It shows abnormal appearing cardiomyocytes having heterogeneous cytoplasm (*H*) (**c**) along with leakage of edema fluid (*arrow heads*) (**a**) and RBCs (*R*) (**d**) from the nearby blood vessels. Numerous fibroblasts (*arrows*) are seen in the interstitium between cardiomyocytes (**b**) (H&E **a** ×400, *Scale bar* = 20 µm; **b**–**d** ×1000, *Scale bar* = 10 µm)

the RHW and the LV wall thickness increased significantly ($p < 0.05$) in the DCM group compared with the control and DCM + ATOR groups without any significant change in the cardiomyocytes diameter (Table 1).

In addition, significant increases ($p < 0.001$) in the CVF and the cleaved caspase-3 percentage area were noticed in DCM group compared with control and DCM + ATOR groups (Fig. 5).

Discussion

In the current study, there was significant increases in the CVF and collagen fibers deposition by the numerous active fibroblasts in the DCM group. This is in concurrence with previous studies (Zhong et al. 2006; Miao et al. 2007; Van Linthout et al. 2007; Wang et al. 2009; Liu et al. 2015). Fibrosis, which characterizes DCM, occurs independent of HTN or CAD and may be associated with myocardial hypertrophy (Huang et al. 2010; Tarquini et al. 2011).

Previous studies have demonstrated that the extensive collagen deposition in DCM is associated with increased expression of connective tissue growth factor (CTGF) and transforming growth factor (TGF)-β (Wang et al. 2009; Mano et al. 2011). In addition, increased formation of advanced glycation end products (AGEs) in hyperglycemia, hastens fibrosis and stiffness in DCM (Falcao-Pires and Leite-Moreira 2012).

Statins can reduce myocardial fibrosis and dysfunction in experimental DCM by inhibition of the overexpressed CTGF and TGF-β resulting in reduction in the interstitial collagen (Wang et al. 2009; Dai et al. 2011). This may explain the restoration of RHW and LV wall thickness to normal values in the DCM + ATOR group, compared with the DCM group in our experiment.

Advanced glycation end products bind covalently to various intra and extracellular proteins. The crosslink in collagen and elastin increases myocardial stiffness, and impairs its relaxation (Petrova et al. 2002; Gawlowski et al. 2009). This results in activation of transcription factors,

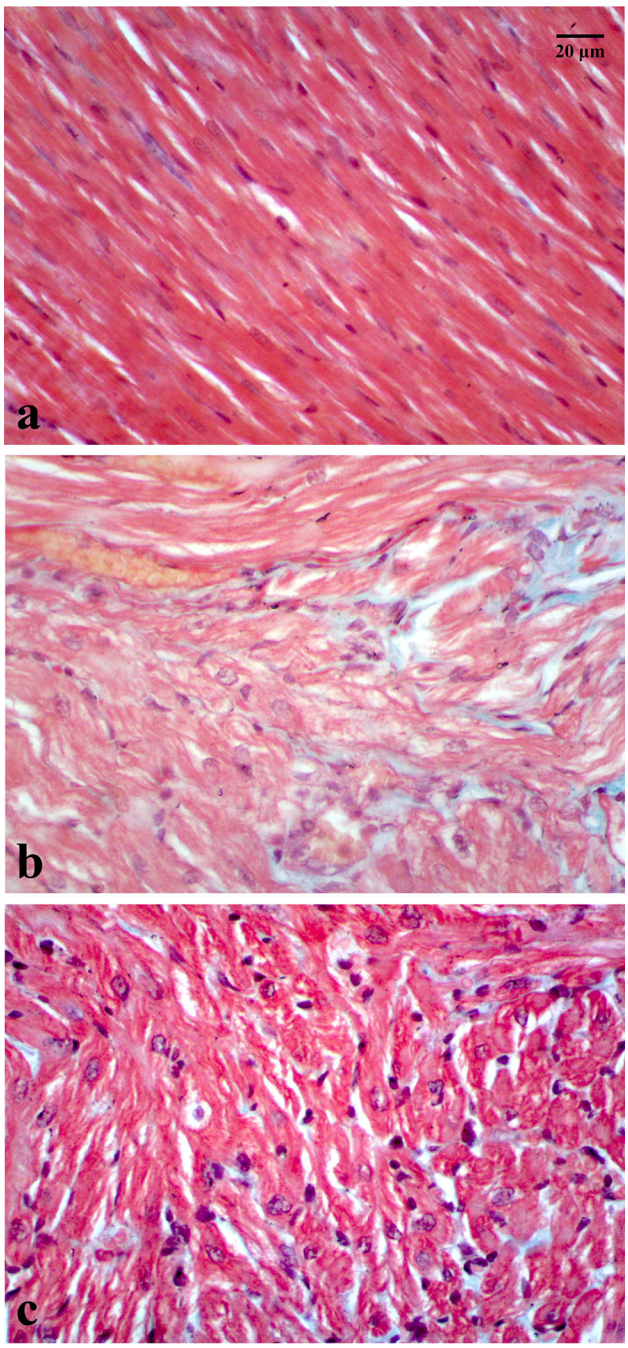

Fig. 3 Representative photomicrographs of LV in all groups stained with Masson's trichrome. Marked increase in the deposited collagen fibers in the interstitium between cardiomyocytes is observed in the DCM group (**b**) compared with minimal ones both in the control (**a**) and DCM + ATOR (**c**) groups (Masson's trichrome ×400, *Scale bar* = 20 µm)

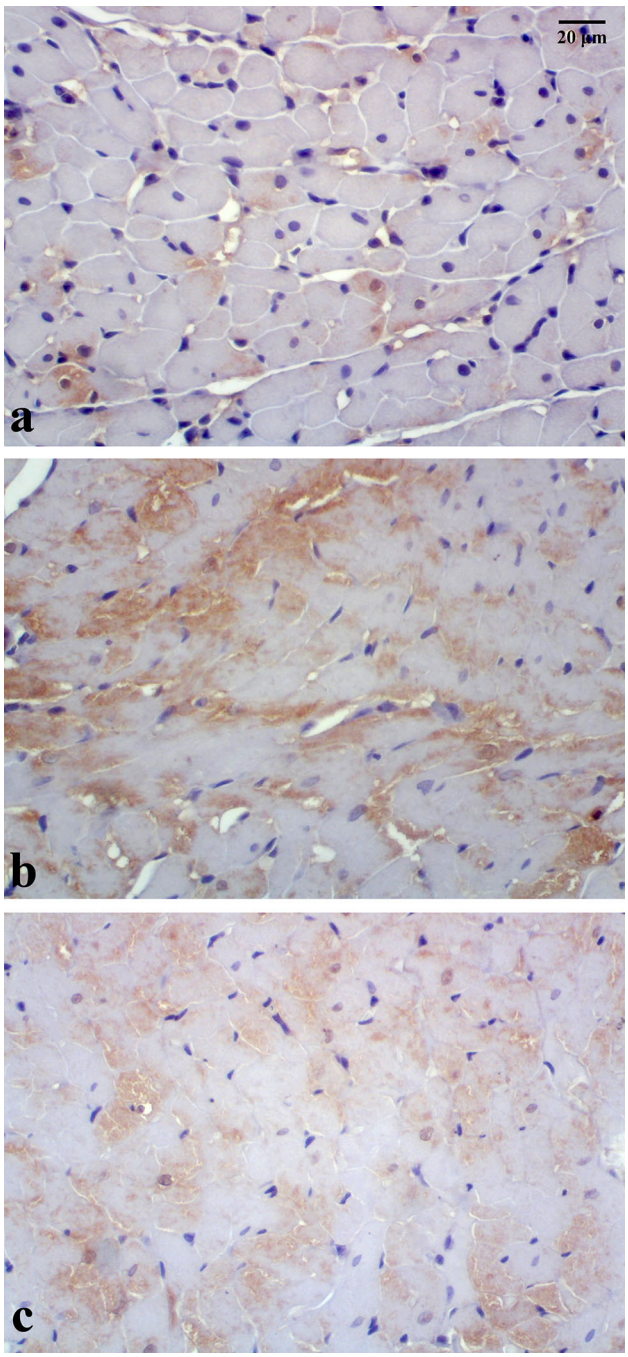

Fig. 4 Representative photomicrographs of LV in all groups stained with anti-cleaved-caspase-3 immunostain. Obvious increase in the caspase-3 expression is detected in the cardiomyocytes of the DCM group (**b**) compared with the minimal expression detected in both the control (**a**) and DCM + ATOR (**c**) groups (Anti-cleaved caspase-3 immunostain ×400, *Scale bar* = 20 µm)

such as nuclear factor-kB (NF-kB) which up-regulates genes that increase the local inflammatory cytokines causing myocardial damage (Burgess et al. 2001; Chen et al. 2008; Guleria et al. 2013; Palomer et al. 2013).

Our data indicated that leakage of edema fluid from the nearby blood vessels and extravasation of RBCs occurred in the DCM group and disappeared in the DCM + ATOR group. This may be attributed to the low-grade

Table 2 Blood glucose (BG) and lipid profile determination in various groups, which includes, serum total cholesterol (TC), high-density lipoprotein cholesterol (HDL), low density lipoprotein cholesterol (LDL), and triglycerides (TG)

	Control	DCM	DCM + ATOR
BG (mg/dl)	112 ± 14	426 ± 31**	418 ± 26**
TC (mg/dl)	79 ± 8	119 ± 24*	125 ± 21*
LDL (mg/dl)	51 ± 13	80 ± 17*	83 ± 15*
HDL (mg/dl)	32 ± 9	30 ± 16	37 ± 14
TG (mg/dl)	46 ± 7	79 ± 12*	82 ± 17*

Values are mean ± SEM

* $p < 0.05$; ** $p < 0.001$ versus control group

inflammation in the myocardium which accompanies the metabolic dysregulation in DCM (Palomer et al. 2013).

Van Linthout et al. (2007) have demonstrated that leucocyte infiltration associates increased cardiac immunostaining of tumor necrosis factor (TNF)-α, interleukin (IL)-1beta, cellular adhesion molecules in DCM. Besides, myocardial mRNA levels of IL-6, TNF-α, CTGF and TGF-β are increased in DCM (Zhong et al. 2006; Mano et al. 2011; Ni et al. 2011). ATOR, independently of its lipid-lowering effect, normalizes diabetes-induced GTP-binding proteins, RAC1 and RHOA, activities which are involved in the DCM-induced inflammation and oxidative stress by increasing phosphorylation of p38 mitogen-activated protein kinase (MAPK; Van Linthout et al. 2007).

A significant increase in the cleaved caspase-3 expression was detected in cardiomyocytes of the DCM group in the current experiment. Caspase-3 expression is increased by hyperglycemia-induced myocardial injury (Cai et al. 2002), pressure overload-induced LVD (Philipp et al. 2004), and in failing hearts (Narula et al. 1999; Scheubel et al. 2002) where it can induce myofibrillar ultrastructural damage (Condorelli et al. 2001). A recent study conducted by Liu et al. (2015) has demonstrated that DM upregulates receptor-interacting protein-3 (RIP_3), a signal molecule involved in TNF-α-mediated apoptosis. On the other hand, suppression of cardiac apoptosis is reported to improve the cardiac structure and function (Xie et al. 2011; Zou and Xie 2013). Interestingly, Chatterjee et al. (2002) claimed that the anti-apoptotic Bcl-2 gene transfer preserves LV function by suppressing cardiac apoptosis.

Moreover, significant increases in the oxidative stress marker, MDA, both in blood and heart tissue were observed in the DCM group and were restored to normal levels in the DCM + ATOR group in our experiment. On the other hand, the antioxidant markers; GSH, GPx, GR and GST were significantly decreased in the DCM group compared with the control and returned to normal values in the DCM + ATOR group.

Hyperglycemia provokes oxidative stress by generation of reactive oxygen species (ROS) or nitrogen species from mitochondria (Cai et al. 2002; Pappachan et al. 2013). NADPH is a co-factor essential for regeneration of reduced glutathione, an important scavenger of ROS. Therefore, increased NADPH utilization in the polyol pathway impairs the cardiomyocyte redox homeostasis (Pappachan et al. 2013). The resultant oxidative stress leads to DNA damage and cardiomyocyte apoptosis (Galvez et al. 2003).

Substances with antioxidant activity such as vitamin E or fluvastatin, reduce myocardial NADPH oxidase subunits and oxidized glutathione which consequently improve LV function in DCM (Hamblin et al. 2007; Shida et al. 2014). Similarly, ATOR decreases DM-induced cardiac lipid peroxide levels, which may be attributed to its pleotropic inhibitory effect on GTP-binding proteins, RAC1 and RHOA (Van Linthout et al. 2007).

In the current study, significant increases in the lipid profile parameters; TC, LDL and TG were detected in both DCM and DCM + ATOR groups. Myocardial steatosis accompanies the increased mitochondrial oxidation and apoptosis in DCM (Ramirez et al. 2013; Zhang and Wei 2013). Hyperglycemia increases the level of free fatty acids (FFA; Falcao-Pires and Leite-Moreira 2012) particularly

Table 3 Determination of serum malondialdehyde (MDA) as well as measurement of LV tissue Levels of MDA, glutathione (GSH), glutathione peroxidase (GPx), glutathione reductase (GR) and glutathione-*S*-transferase (GST) in various groups

	Control	DCM	DCM + ATOR
Blood MDA (nmol/dl)	1.47 ± 0.03	3.28 ± 0.48**,##	1.52 ± 0.08
Heart MDA (nmol/g)	49.17 ± 3.46	68.24 ± 4.72*,#	52.32 ± 4.86
GSH (μg/g)	207.95 ± 8.63	162.74 ± 9.68*,#	198.75 ± 14.49
GPx (μmol NADPH/min/mg protein	0.156 ± 0.0072	0.092*,#	0.153 ± 0.0047
GR (μmol NADPH/min/mg protein	16.25 ± 1.31	11.37 ± 1.42*,#	15.89 ± 1.26
GST (μmol CDNB conjugated/min/mg protein)	11.87 ± 0.82	7.24 ± 1.63*,#	10.73 ± 1.78

Values are mean ± SEM; CDNB 1-chloro-2,4-dinitrobenzene

* $p < 0.05$; ** $p < 0.001$ versus control group

# $p < 0.05$; ## $p < 0.001$ versus DCM + ATOR group

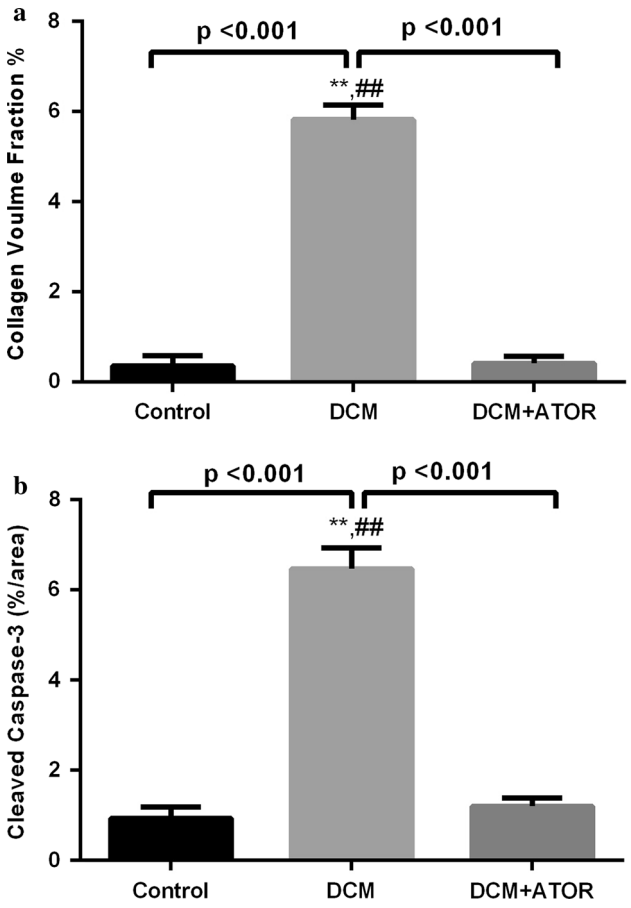

Fig. 5 Histograms of the collagen volume fraction (CVF) (**a**) and cleaved caspase-3 percentage area (**b**) in various groups. $^{**}p < 0.001$ versus control group. $^{\#\#}p < 0.001$ versus DCM + ATOR group

the saturated FA, palmitate, which causes accumulation of the toxic intermediate, ceramide (Pappachan et al. 2013).

Cardiomyocyte accumulation of palmitate, ceramide and TG enhances oxidative stress, apoptosis as well as cardiac hypertrophy and dysfunction (Guleria et al. 2013; Pappachan et al. 2013; Palomer et al. 2013; Ramirez et al. 2013). This also may account for the pale areas inside cardiomyocytes observed in DCM group in the current study.

In addition, an obvious increase in the capillary number in the DCM + ATOR group was observed in the current study. Similar finding was observed by Shida et al. (2014) who mentioned that this beneficial effect of statins may be attributed to the reduction in myocardial oxidative stress and upregulation of angiogenic factors that can overcome endothelial destruction in DCM (Danilova et al. 2015). In parallel, statins increase myocardial endothelial nitric oxide synthase, vascular endothelial growth factor, and hypoxia-inducible factor-1α mRNA expression (Van Linthout et al. 2007; Shida et al. 2014) which may explain the noticeable improvement in the coronary microcirculation.

Conclusion

It is concluded that administration of atorvastatin in experimental diabetic cardiomyopathy can efficiently preserve the myocardial structure nearly similar to normal conditions. This effect can be considered as a non-lipid lowering benefit of statins and may be attributed to the suppression of both hyperglycemia-induced apoptosis as well as the associated oxidative stress.

Conflict of interest There is no conflict of interest.

References

Beutler E, Duron O, Kelly BM (1963) Improved method for the determination of blood glutathione. J Lab Clin Med 61:882–888

Burgess ML, McCrea JC, Hedrick HL (2001) Age-associated changes in cardiac matrix and integrins. Mech Ageing Dev 122: 1739–1756

Cai L, Li W, Wang G et al (2002) Hyperglycemia-induced apoptosis in mouse myocardium: mitochondrial cytochrome C-mediated caspase-3 activation pathway. Diabetes 51:1938–1948

Cai L, Wang Y, Zhou G et al (2006) Attenuation by metallothionein of early cardiac cell death via suppression of mitochondrial oxidative stress results in a prevention of diabetic cardiomyopathy. J Am Coll Cardiol 48:1688–1697

Chatterjee S, Stewart AS, Bish LT et al (2002) Viral gene transfer of the antiapoptotic factor Bcl-2 protects against chronic postischemic heart failure. Circulation 106:I-212–I-217

Chen B, Zhang Y, Liu G et al (2008) Effects of valsartan, mycophenolate mofetil and their combined application on TRAIL and nuclear factor-kappaB expression in the kidneys of diabetic rats. Zhonghua yi xue za zhi 88:540–545

Chen YH, Feng B, Chen ZW (2012) Statins for primary prevention of cardiovascular and cerebrovascular events in diabetic patients without established cardiovascular diseases: a meta-analysis. Exp Clin Endocrinol Diabetes 120:116–120

Condorelli G, Roncarati R, Ross J et al (2001) Heart-targeted overexpression of caspase3 in mice increases infarct size and depresses cardiac function. Proc Natl Acad Sci USA 98: 9977–9982

Dai Q-M, Lu J, Liu N-F (2011) Fluvastatin attenuates myocardial interstitial fibrosis and cardiac dysfunction in diabetic rats by inhibiting over-expression of connective tissue growth factor. Chin Med J (Engl) 124:89–94

Danilova IG, Sarapultsev PA, Medvedeva SU et al (2015) Morphological restructuring of myocardium during the early phase of experimental diabetes mellitus. Anat Rec (Hoboken, NJ: 2007) 298:396–407

Duncan JG (2011) Mitochondrial dysfunction in diabetic cardiomyopathy. Biochim Biophys Acta 1813:1351–1359

Falcao-Pires I, Leite-Moreira AF (2012) Diabetic cardiomyopathy: understanding the molecular and cellular basis to progress in diagnosis and treatment. Heart Fail Rev 17:325–344

Galvez AS, Ulloa JA, Chiong M et al (2003) Aldose reductase induced by hyperosmotic stress mediates cardiomyocyte apoptosis: differential effects of sorbitol and mannitol. J Biol Chem 278:38484–38494

Gawai KR, Pawar SS (1984) Purification and characterization of glutathione-*S*-transferase from liver cytosol of phenobarbital-treated rabbits. Xenobiotica 14:605–607

Gawlowski T, Stratmann B, Stork I et al (2009) Heat shock protein 27 modification is increased in the human diabetic failing heart. Horm Metab Res 41:594–599

Guleria RS, Singh AB, Nizamutdinova IT et al (2013) Activation of retinoid receptor-mediated signaling ameliorates diabetes-induced cardiac dysfunction in Zucker diabetic rats. J Mol Cell Cardiol 57:106–118

Hamblin M, Smith HM, Hill MF (2007) Dietary supplementation with vitamin E ameliorates cardiac failure in type I diabetic cardiomyopathy by suppressing myocardial generation of 8-iso-prostaglandin F2alpha and oxidized glutathione. J Card Fail 13:884–892

Huang YQ, Wang X, Kong W (2010) Diabetic cardiomyopathy. Sheng li ke xue jin zhan [Progress in physiology] 41:31–36

Huynh K, Bernardo BC, McMullen JR et al (2014) Diabetic cardiomyopathy: mechanisms and new treatment strategies targeting antioxidant signaling pathways. Pharmacol Ther 142:375–415

Konduracka E, Cieslik G, Galicka-Latala D et al (2013) Myocardial dysfunction and chronic heart failure in patients with long-lasting type 1 diabetes: a 7-year prospective cohort study. Acta Diabetol 50:597–606

Lim SH, Lee J (2012) Methanol extract of Cassia mimosoides var. nomame attenuates myocardial injury by inhibition of apoptosis in a rat model of ischemia-reperfusion. Prev Nutr Food Sci 17:177–183

Lim SH, Kim MY, Lee J (2014) Apple pectin, a dietary fiber, ameliorates myocardial injury by inhibiting apoptosis in a rat model of ischemia/reperfusion. Nutr Res Pract 8:391–397

Liu YS, Huang ZW, Wang L et al (2015) Sitagliptin alleviated myocardial remodeling of the left ventricle and improved cardiac diastolic dysfunction in diabetic rats. J Pharmacol Sci 127: 260–274

Long WK, Carson PE (1961) Increased erythrocyte glutathione reductase activity in diabetes mellitus. Biochem Biophys Res Commun 5:394–399

Mano Y, Anzai T, Kaneko H et al (2011) Overexpression of human C-reactive protein exacerbates left ventricular remodeling in diabetic cardiomyopathy. Circ J 75:1717–1727

Miao Y, Zhang W, Zhong M et al (2007) Activation of transforming growth factor-beta1/Smads signal pathway in diabetic cardiomyopathy and effects of valsartan thereon: experiment with rats. Zhonghua yi xue za zhi 87:366–370

Narula J, Pandey P, Arbustini E et al (1999) Apoptosis in heart failure: release of cytochrome c from mitochondria and activation of caspase-3 in human cardiomyopathy. Proc Natl Acad Sci USA 96:8144–8149

Ni Q, Wang J, Li EQ et al (2011) Study on the protective effect of shengmai san (see text) on the myocardium in the type 2 diabetic cardiomyopathy model rat. Journal of traditional Chinese medicine = Chung i tsa chih ying wen pan/sponsored by All-China Association of Traditional Chinese Medicine. Acad Tradit Chin Med 31:209–219

Ouyang C, You J, Xie Z (2014) The interplay between autophagy and apoptosis in the diabetic heart. J Mol Cell Cardiol 71:71–80

Paglia DE, Valentine WN (1967) Studies on the quantitative and qualitative characterization of erythrocyte glutathione peroxidase. J Lab Clin Med 70:158–169

Palomer X, Salvado L, Barroso E et al (2013) An overview of the crosstalk between inflammatory processes and metabolic dysregulation during diabetic cardiomyopathy. Int J Cardiol 168:3160–3172

Pappachan JM, Varughese GI, Sriraman R et al (2013) Diabetic cardiomyopathy: pathophysiology, diagnostic evaluation and management. World J Diabetes 4:177–189

Petrova R, Yamamoto Y, Muraki K et al (2002) Advanced glycation endproduct-induced calcium handling impairment in mouse cardiac myocytes. J Mol Cell Cardiol 34:1425–1431

Philipp S, Pagel I, Hohnel K et al (2004) Regulation of caspase 3 and Fas in pressure overload-induced left ventricular dysfunction. Eur J Heart Fail 6:845–851

Picatoste B, Ramirez E, Caro-Vadillo A et al (2013) Sitagliptin reduces cardiac apoptosis, hypertrophy and fibrosis primarily by insulin-dependent mechanisms in experimental type-II diabetes. Potential roles of GLP-1 isoforms. PLoS ONE 8:e78330

Ramirez E, Klett-Mingo M, Ares-Carrasco S et al (2013) Eplerenone attenuated cardiac steatosis, apoptosis and diastolic dysfunction in experimental type-II diabetes. Cardiovasc Diabetol 12:172

Scheubel RJ, Bartling B, Simm A et al (2002) Apoptotic pathway activation from mitochondria and death receptors without caspase-3 cleavage in failing human myocardium: fragile balance of myocyte survival? J Am Coll Cardiol 39:481–488

Schilling JD, Mann DL (2012) Diabetic cardiomyopathy: bench to bedside. Heart Fail Clin 8:619–631

Shida T, Nozawa T, Sobajima M et al (2014) Fluvastatin-induced reduction of oxidative stress ameliorates diabetic cardiomyopathy in association with improving coronary microvasculature. Heart Vessels 29:532–541

Sun M, Dawood F, Wen WH et al (2004) Excessive tumor necrosis factor activation after infarction contributes to susceptibility of myocardial rupture and left ventricular dysfunction. Circulation 110:3221–3228

Tarquini R, Lazzeri C, Pala L et al (2011) The diabetic cardiomyopathy. Acta Diabetol 48:173–181

Taylor F, Huffman MD, Macedo AF et al (2013) Statins for the primary prevention of cardiovascular disease. Cochrane Database Syst Rev 1:Cd004816

Tietz NW, Burtis CA, Ashwood ER (2006) Tietz textbook of clinical chemistry and molecular diagnostics. Elsevier, St. Louis

Van Linthout S, Riad A, Dhayat N et al (2007) Anti-inflammatory effects of atorvastatin improve left ventricular function in experimental diabetic cardiomyopathy. Diabetologia 50: 1977–1986

Wang YJ, Fu GS, Chen FM et al (2009) The effect of valsartan and fluvastatin on the connective tissue growth factor expression in experimental diabetic cardiomyopathy. Zhonghua nei ke za zhi 48:660–665

Xie Z, He C, Zou MH (2011) AMP-activated protein kinase modulates cardiac autophagy in diabetic cardiomyopathy. Autophagy 7:1254–1255

Xue D, Shaham S, Horvitz HR (1996) The Caenorhabditis elegans cell-death protein CED-3 is a cysteine protease with substrate specificities similar to those of the human CPP32 protease. Genes Dev 10:1073–1083

Zhang YL, Wei JR (2013) 3-nitrotyrosine, a biomarker for cardiomyocyte apoptosis induced by diabetic cardiomyopathy in a rat model. Mol Med Rep 8:989–994

Zhong M, Zhang Y, Miao Y et al (2006) Mechanism of reversion of myocardial interstitial fibrosis in diabetic cardiomyopathy by valsartan. Zhonghua yi xue za zhi 86:232–236

Zidar N, Dolenc-Strazar Z, Jeruc J et al (2006) Immunohistochemical expression of activated caspase-3 in human myocardial infarction. Virchows Arch Int J Pathol 448:75–79

Zou MH, Xie Z (2013) Regulation of interplay between autophagy and apoptosis in the diabetic heart: new role of AMPK. Autophagy 9:624–625